Journal of Thermal Engineering
https://jten.yildiz.edu.tr/
https://doi.org/10.47481/jten.0077

RESEARCH ARTICLE

Radial basis function neural network modelling and multi-objective optimization of heat transfer performance in perforated fins under forced convection

Wadhah Hussein Al Doori[1,*], Hasan Koten[2]

[1]Energy Department, Natural Resources Research Center, Tikrit University, Tikrit 3400, Saladin, Iraq
[2]Istanbul Medeniyet University, Mechanical Engineering Department, 34700, Istanbul, Turkey

Abstract

Efficient thermal management stays a critical requirement in aerospace systems, high-power electronics, and compact heat exchangers, where excessive temperature rise can degrade performance and reliability. Conventional solid fins are limited by boundary-layer development and structural weight, motivating the use of perforated fins to enhance convective heat transfer while reducing material usage. This study develops a computational framework that combines high-fidelity computational fluid dynamics (CFD), Radial Basis Function Neural Network (RBFNN) surrogate modeling, and multi-objective optimization to investigate the thermo-fluid performance of perforated fins under forced convection. The aims are to maximize heat transfer performance, represented by the Nusselt number (Nu), and minimize hydraulic losses, represented by pressure drop (ΔP), while considering perforation number, perforation diameter, and airflow velocity as design variables. The RBFNN model was trained using CFD-generated data and confirmed against independent test datasets, showing high predictive accuracy ($R^2 > 0.98$) with low prediction error. It is important to note that validation in this study is limited to comparison with CFD results and previously published experimental correlations [4] and does not involve new experimental measurements. The multi-objective optimization, performed using NSGA-II, produced a Pareto frontier illustrating the trade-off between thermal enhancement and pressure loss. The optimized configurations achieved up to 16% improvement in heat transfer compared to a solid fin baseline, along with approximately 24% reduction in material usage. Sensitivity analysis using Sobol indices found airflow velocity as the dominant parameter, contributing approximately 60% to performance variation. The proposed framework provides a computationally efficient approach for exploring perforated fin designs and supports engineering decision-making under competing thermal and hydraulic aims.

Keywords: Radial basis function neural network, perforated fins, multi-objective optimization, heat transfer enhancement, surrogate modeling

Cite this article as: Al Doori, W. H., & Koten, H. (2026). Radial basis function neural network modelling and multi-objective optimization of heat transfer performance in perforated fins under forced convection. Journal of Thermal Engineering, 12(6), 1955–1965. https://doi.org/10.47481/jten.0077

1. Introduction

Efficient thermal management is essential in a wide range of engineering applications, including aerospace systems, power electronics, and compact heat exchangers, where excessive temperature rise can reduce system reliability and operational efficiency. Extended surfaces such as fins are commonly used to enhance convective heat transfer. However, conventional solid fins are often limited by boundary-layer development and increased structural weight, particularly under forced convection conditions [1], [2]. Improving heat transfer performance while minimizing material usage stays a key engineering challenge. Perforated fins have been proposed as an effective alternative due to their ability to disrupt boundary layers, promote flow mixing, and reduce material volume. Previous experimental and numerical studies have demonstrated that introducing perforations can enhance heat transfer performance, with reported improvements depending on perforation geometry, size, and arrangement [3]–[6]. For instance, rectangular perforations have been shown to increase heat transfer by approximately 16% under forced convection conditions while simultaneously reducing fin mass [7]. However, most existing studies are limited to fixed operating conditions or single-parameter investigations, which restrict the ability to

*Corresponding Author
E-mail Adress: wadhah.h.abdulrzzaq@tu.edu.iq

Submitted: 12 December 2025; **Accepted:** 8 June 2026

This paper was recommended for publication in revised form by Editor-in-Chief Ahmet Selim Dalkılıç

explore complex interactions between geometric and flow variables. In parallel, data-driven modeling approaches have been increasingly applied in thermo-fluid systems. Artificial neural networks have been used to predict heat transfer coefficients and pressure drop in various configurations [8]–[12]. Among these methods, Radial Basis Function Neural Networks (RBFNN) are particularly suitable for nonlinear regression problems due to their fast training and smooth interpolation characteristics [13]–[15]. Nevertheless, most studies employing neural networks focus on forward prediction rather than design optimization, and only a limited number of works integrate surrogate modeling with geometric design exploration.

Multi-objective optimization techniques provide a systematic framework for addressing competing design aims, such as maximizing heat transfer while minimizing pressure drop. Evolutionary algorithms, such as the Non-dominated Sorting Genetic Algorithm II (NSGA-II), have been widely used in engineering optimization problems [15]. However, in the context of perforated fins, most studies rely either on direct CFD-based parametric analysis or single-objective optimization approaches [16], without fully exploiting surrogate-assisted multi-objective optimization.

1.1. Comparison with recent studies and research gap

Recent studies have explored perforated fin systems using numerical or experimental approaches [17]–[21], focusing primarily on thermal performance enhancement through geometric modification. While these studies offer valuable insights, they generally lack integration of surrogate modeling, uncertainty quantification, and global sensitivity analysis within a unified framework. In addition, existing surrogate-based studies often emphasize prediction accuracy without incorporating multi-objective optimization or uncertainty propagation.

To address this limitation, Table 1 provides a comparative overview of representative studies, highlighting the absence of integrated frameworks that combine CFD, surrogate modeling, multi-objective optimization, sensitivity analysis, and uncertainty quantification for perforated fin systems.

Table 1. Comparative analysis of surrogate-assisted optimization studies in perforated fin and related thermo-fluid systems

Study	Method	Application	Multi-Objective	Uncertainty Quantification	Sensitivity Analysis
Al Doori [2], [22]	Experimental + Numerical	Perforated pin fins	No	No	No
Ibrahim et al. [4]	Experimental + Numerical	Square perforated fins	No	No	No
Awasarmol et al. [5]	Experimental	Perforated fin arrays	No	No	No
Shaeri et al. [23]	Numerical (CFD)	Lateral perforated fin heat sinks	No	No	No
Sözbir & Ekmekçi [8]	ANN only	Forced convection in ducts	No	No	No
Xie et al. [9]	ANN only	Shell-and-tube heat exchangers	No	No	No
Tandiroglu [10]	ANN only	Transient forced convection	No	No	No
Cao et al. [15]	RBFNN + GA	Laser welding (non-thermal)	No	No	No
Zhang & Luo (2025) [17]	Numerical (CFD)	Elliptical perforated fin heat exchangers	No	No	No
Haque et al. (2025) [18]	Numerical (RANS k-ε)	Twisted & perforated forked pin fin heat sink	No	No	No
Noori & Saeed (2025) [19]	Experimental + CFD	Radial-shaped perforated fins	No	No	No
Zohora et al. (2025) [20]	Numerical (realizable κ-ε)	Perforated pin fin heat sinks	No	No	No
Yusuf & Bhatti (2026) [21]	Numerical (Collocation method)	Non-thermal plasma + photocatalytic hybrid nanofluid flow	No	No	No
Present Study	RBFNN + NSGA-II + Sobol + Monte Carlo UQ	Perforated fins under forced convection	Yes (Nu vs. ΔP)	Yes (95% CI via Monte Carlo + GCI)	Yes (first-order + total-order indices)

1.2. Novelty and contribution

The present study contributes to literature by developing an integrated computational framework for the analysis and optimization of perforated fins under forced convection. The main contributions are summarized as follows:

- Integration of CFD simulations with RBFNN surrogate modeling for efficient prediction of thermo-fluid performance.
- Application of multi-objective optimization (NSGA-II) to simultaneously maximize Nusselt number and minimize pressure drop.
- Incorporation of Sobol-based global sensitivity analysis to quantify parameter influence and interaction effects.
- Inclusion of Monte Carlo-based uncertainty quantification to assess robustness under operational variability.

Unlike earlier studies that focus either on parametric analysis or predictive modeling, the present work combines these elements within a single workflow, enabling systematic exploration of design trade-offs.

1.3. Clarification of multi-objective formulation

The optimization problem in this study is defined using two competing objective functions:

- Objective 1 (Thermal performance): Maximize Nusselt number (Nu)
- Objective 2 (Hydraulic performance): Minimize pressure drop (ΔP)

These aims are the fundamental trade-off in forced convection systems, where increased heat transfer is typically associated with higher flow resistance. The decision variables considered in the optimization are:

- Airflow velocity (u)
- Perforation number (N)
- Perforation diameter (d)

This formulation allows identification of Pareto-optimal solutions that balance thermal efficiency and hydraulic performance.

1.4. Validation and reliability considerations

The predictive capability of the proposed framework is evaluated through comparison between RBFNN predictions and CFD-generated data, as well as benchmarking against previously published experimental results [4]. It should be noted that no new experimental validation is performed in this study. Therefore, the results should be interpreted as numerically confirmed within the investigated parameter space rather than experimentally confirmed.

1.5. Scope and structure of the study

Based on the identified research gap, this study develops a computational method that integrates CFD simulations, RBFNN surrogate modeling, Sobol sensitivity analysis, NSGA-II optimization, and uncertainty quantification. The framework is applied to investigate the thermo-fluid behavior of perforated fins under forced convection, with emphasis on performance improvement and design trade-offs.

2. Methodology

2.1. Overview of the computational framework

This study develops an integrated computational framework for analyzing and perfecting the thermo-fluid performance of perforated fins under forced convection. The framework combines:

- High-fidelity Computational Fluid Dynamics (CFD) simulations
- Radial Basis Function Neural Network (RBFNN) surrogate modeling
- Multi-objective optimization using NSGA-II
- Global sensitivity analysis based on Sobol indices
- Uncertainty quantification using Monte Carlo simulation

The CFD model is used to generate the dataset, while the RBFNN surrogate replaces repeated CFD evaluations during optimization, significantly reducing computational costs.

2.2. Physical model and assumptions

The perforated fin system is modeled under steady-state forced convection with the following assumptions:

- Three-dimensional, steady-state flow
- Newtonian, incompressible fluid
- Constant thermophysical properties
- Negligible radiation heat transfer
- Negligible buoyancy effects
- No thermo-mechanical deformation

A constant heat flux is applied at the fin base, while all other external surfaces are treated as adiabatic.

The parameters investigated include:

- Air velocity: $u=0.4–1.8\,m/s$
- Perforation diameter: $d=8–22.5\,mm$
- Perforation number: $N=4–15$
- Perforation shapes: circular, square, and rectangular

The corresponding Reynolds number range is:

$$Re = \frac{\rho u D_h}{\mu} \approx 1.8 \times 10^3 \text{ to } 5.7 \times 10^3$$

which lies in the transitional to moderately turbulent regime typical of compact air-cooled systems.

2.3. Governing equations

The flow and heat transfer are governed by the steady-state Reynolds-Averaged Navier–Stokes (RANS) equations coupled with the energy equation.

2.3.1. Continuity equation

$$\nabla \cdot \vec{v} = 0 \tag{1}$$

2.3.2. Momentum equation (RANS form)

$$\rho(\vec{v} \cdot \nabla)\vec{v} = -\nabla p + \nabla \cdot [(\mu + \mu_t)\nabla \vec{v}] \tag{2}$$

where μ_t is the turbulent eddy viscosity.

2.3.3. Energy equation

$$\rho c_p(\vec{v} \cdot \nabla T) = \nabla \cdot [(k + k_t)\nabla T] \tag{3}$$

where is the turbulent thermal conductivity.

2.4. Turbulence modeling

The RNG k–ε turbulence model is used to be turbulence effects.

Turbulent Kinetic Energy Equation:

$$\rho(\vec{v} \cdot \nabla k) = \nabla \cdot \left[\left(\mu + \frac{\mu_t}{\sigma_k}\right)\nabla k\right] + G_k - \rho\epsilon \tag{4}$$

Dissipation Rate Equation:

$$\rho(\vec{v} \cdot \nabla \epsilon) = \nabla \cdot \left[\left(\mu + \frac{\mu_t}{\sigma_\epsilon}\right)\nabla \epsilon\right] + C_{1\epsilon}\frac{\epsilon}{k}G_k - C_{2\epsilon}\rho\frac{\epsilon^2}{k} \tag{5}$$

Turbulent Viscosity:

$$\mu_t = \rho C_\mu \frac{k^2}{\epsilon} \tag{6}$$

Justification and Limitations:

The RNG k–ε model is selected due to:

- Improved performance in separated and recirculating flows
- Lower computational cost compared to SST k–ω and LES

However, it has limitations:

- Reduced accuracy in transitional regimes
- Inability to resolve transient vortex structures
- Dependence on wall functions

These limitations are acknowledged and considered acceptable for comparative design analysis.

2.5. Boundary conditions

The CFD simulations are performed with the following boundary conditions:

Inlet: Uniform velocity profile

$$u = 0.4 - 1.8\frac{m}{s}, T = T_\infty$$

Outlet: Pressure outlet

$$p = 0\,\text{Pa. (gauge)}$$

Fin Base: Constant heat flux

$$q'' = 70 - 85\,\text{kW/m}^2$$

Solid Walls: No-slip condition

$$u = v = w = 0$$

Other Surfaces: Adiabatic condition

$$\frac{\partial T}{\partial n} = 0$$

Symmetry Planes (if applicable): Zero normal gradients

These conditions are realistic forced convection cooling scenarios in compact heat exchangers.

2.6. Performance parameters and dimensionless quantities

Nusselt Number:

$$Nu = \frac{hD_h}{k} \tag{7}$$

where is the convective heat transfer coefficient.

Pressure Drop:

$$\Delta P = P_{in} - P_{out} \tag{8}$$

Fin Efficiency:

$$\eta_f = \frac{\text{Actual heat transfer}}{\text{Ideal heat transfer}} \tag{9}$$

Importance of Dimensionless Parameters:

Dimensionless parameters such as Reynolds number and Nusselt number enable:

- Generalization of results
- Comparison across different systems
- Reduction of scaling effects

2.7. Grid independence and numerical accuracy

A grid independence study was conducted using progressively refined meshes (Table 1). Convergence was achieved when variations in heat transfer coefficient became negligible.

Grid Convergence Index (GCI):

$$GCI = \frac{[F_s\,|\,\phi_1 - \phi_2\,|]}{|\phi_1(r^p - 1)|} \times 100\% \tag{10}$$

where:

$F_s = 1.25$ (safety factor), r is refinement ratio, P is order of accuracy

The computed GCI ≈ 1.3% confirms low discretization error.

2.8. Surrogate model development (RBFNN)

The RBFNN model maps input variables to outputs:

Inputs: x= (Re, N, d/D, q″, shape)

Outputs: (Nu, ΔP)

RBFNN Function

$$y(x) = \sum_{i=1}^{M} w_i \exp\left(-\frac{\| x - c_i \|^2}{2\sigma_i^2}\right) \tag{11}$$

where:

w_i : weights, : c_i centers, σ_i: spread

The dataset was split into:

80% training, 20% testing

with 5-fold cross-validation to ensure robustness.

2.9. Multi-objective optimization formulation (clarified)

The optimization problem is defined as:

$$\text{Maximize } f_1(x) = Nu(x) \tag{12}$$

$$\text{Minimize } f_2(x) = \Delta P(x) \tag{13}$$

where:

$$x = (u, N, d)$$

The optimization is performed using NSGA-II with:

Population size = 100

Generations = 200

Crossover probability = 0.9

Mutation probability = 0.1

2.10. Sensitivity analysis

Sobol indices are used to quantify parameter influence:

$$S_i = \frac{V_i}{V_{Total}} \tag{14}$$

where V_i is partial variance of input .

2.11. Uncertainty quantification

Monte Carlo simulation is used to propagate uncertainties:

- Velocity: ±5%
- Diameter: ±1 mm
- Thermal conductivity: 190–220 W/m·K

Resulting outputs are expressed as:

3. Results and discussion

3.1. Surrogate model performance and validation

The predictive capability of the Radial Basis Function Neural Network (RBFNN) surrogate model was evaluated using both training and independent test datasets derived from CFD simulations. The model achieved high accuracy, with coefficients of determination exceeding 0.98 for both datasets, showing strong agreement between predicted and simulated values of Nusselt number (Nu) and pressure drop (ΔP).

Figure 1 presents the parity plot comparing CFD-computed and RBFNN-predicted Nusselt numbers over the investigated parameter ranges (air velocity u=0.4–1.8 m/s, perforation number N=4–15, and diameter d=8–22.5 mm). The close alignment of data points along the 45° line confirms that the surrogate accurately captures the nonlinear thermo-fluid response.

The error distributions shown in Figures 2 and 3 further show that most prediction errors stay below 1%, proving consistent accuracy across the design space rather than localized agreement. Cross-validation results also showed minimal variance in model performance, confirming that the surrogate model is stable and not sensitive to dataset partitioning.

It should be emphasized that validation in this study is limited to comparison with CFD-generated data and previously reported experimental trends [4]. Therefore, the surrogate model is considered reliable within the investigated parameter space but not externally confirmed through new experimental measurements.

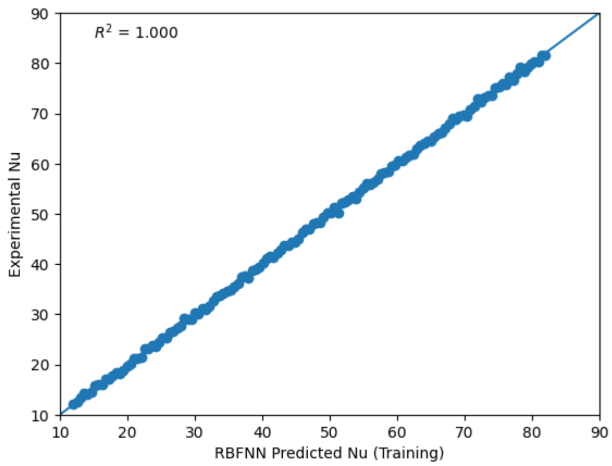

Figure 1. CFD-computed versus RBFNN-predicted average Nusselt number (training dataset)

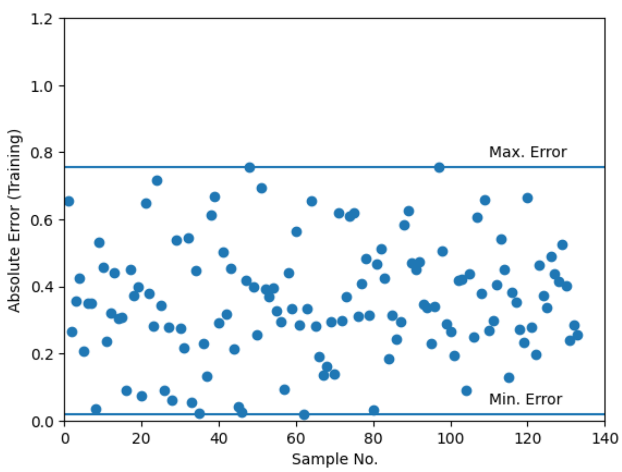

Figure 2. Absolute prediction error distribution for the training dataset

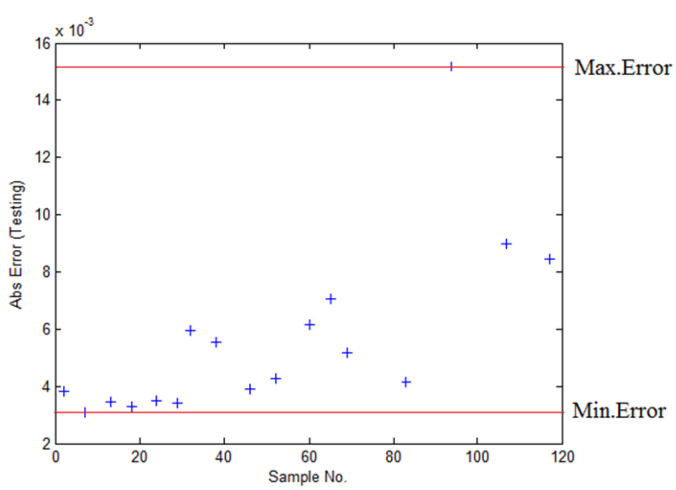

Figure 3. Relative prediction error distribution for the test dataset

2.9. Multi-objective optimization and pareto analysis

The integration of the RBFNN surrogate with the NSGA-II algorithm enabled efficient exploration of the design space and identification of Pareto-optimal solutions. The resulting Pareto front, shown in Figure 4, illustrates the trade-off between heat transfer enhancement (Nu) and pressure drop (ΔP).

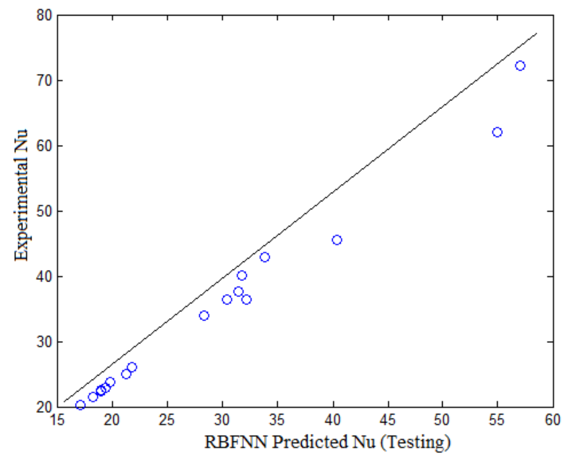

Figure 4. Pareto front of Nu versus ΔP (NSGA-II results)

Each point on the Pareto frontier corresponds to a specific combination of design variables within the defined ranges:

- Air velocity: u=0.4–1.8 m/s
- Perforation number: N=4–15
- Perforation diameter: d=8–22.5 mm

The Pareto curve shows a monotonic trend, where higher Nusselt numbers are associated with increased pressure drop. This behavior reflects the inherent coupling between enhanced convective mixing and increased flow resistance.

At the high-performance end of the Pareto front, a configuration with fifteen rectangular perforations at u=1.8 m/s achieved a Nusselt number of approximately 66.2, accompanied by a pressure drop of 12.3 Pa. In contrast, a low-resistance configuration with six circular perforations at u=0.7 m/s resulted in a lower Nusselt number of approximately 38.1 with a pressure drop of 3.9 Pa.

These results define the performance envelope of the system and prove that no single configuration simultaneously perfects both aims. Instead, the Pareto front provides a set of possible solutions that can be selected based on application-specific requirements, such as maximizing heat transfer or minimizing pumping power.

An intermediate configuration with moderate perforation density and diameter offers a balanced compromise, achieving improved thermal performance with acceptable pressure penalty. This type of solution is particularly relevant for practical applications where both thermal efficiency and energy consumption must be considered.

3.3. Comparison with baseline and performance enhancement

To quantify the effectiveness of perforation, the optimized configurations were compared with a solid fin baseline (Table 2). The results show that perforated fins can achieve up to 16% enhancement in heat transfer performance, accompanied by approximately 24% reduction in material usage.

Table 2. Performance comparison between baseline and perfected perforated configurations

Configuration	Nu	ΔP (Pa)	Mass Reduction (%)
Solid Fin	57.0	5.2	0
Low-Drag Design	38.1	3.9	12
Optimal Design	66.2	12.3	24

Figure 5 illustrates the comparison between the baseline and optimized configuration. The increase in Nusselt number reflects improved convective heat transfer due to flow disruption and enhanced mixing, while the reduction in mass results from material removal through perforations.

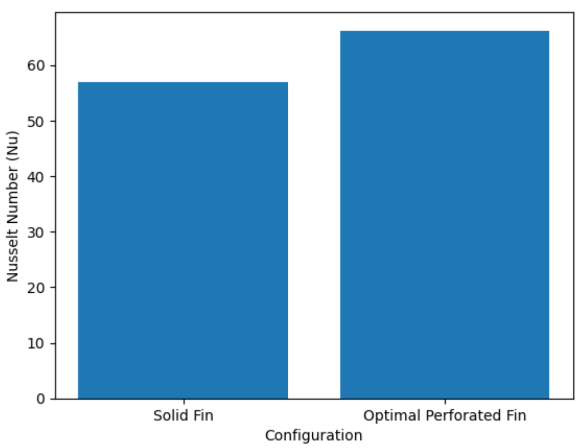

Figure 5. Comparison of Nusselt number between the solid fin and the optimized perforated configuration

Although the magnitude of improvement may appear moderate, it is consistent with previously reported experimental and numerical studies [4], [23, 24], where enhancements typically range between 10% and 25%. This agreement supports the physical plausibility of the results obtained.

3.4. Sensitivity analysis and parameter influence

Global sensitivity analysis was performed using Sobol indices to quantify the contribution of each design variable to the variance in Nusselt number. The results, shown in Figures 6 and 7, show that airflow velocity is the dominant parameter, accounting for approximately 60% of the total variance.

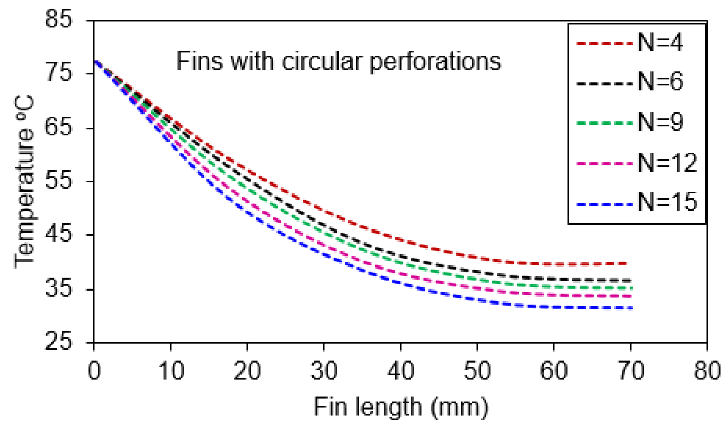

Figure 6. First-order Sobol indices showing parameter influence on Nu

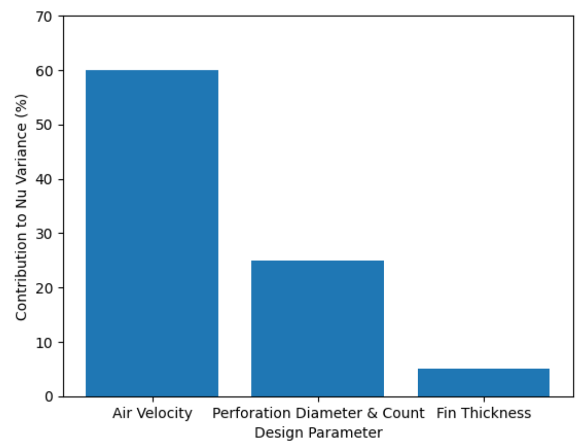

Figure 7. Global Sobol sensitivity indices showing contribution of design parameters to Nu variance

Perforation diameter and perforation number contribute approximately 25% collectively, including interaction effects. The remaining variance is attributed to higher-order interactions and minor parameters.

This distribution reflects the fundamental role of Reynolds number in forced convection heat transfer. As air flow velocity increases, convective transport is enhanced, leading to higher Nusselt numbers. In contrast, geometric parameters primarily influence local flow structures and boundary-layer behavior.

The sensitivity results offer important design insight: optimization efforts should prioritize airflow management before fine-tuning geometric parameters. This finding also explains the steep slope saw in the Pareto front, where increases in velocity simultaneously improve heat transfer and increase pressure drop.

3.5. Flow and thermal field analysis

The temperature contour plots presented in Figures 8–11 provide insight into the physical mechanisms responsible for the observed performance trends. Under identical operating conditions (N=6, u=1.2 m/s), distinct differences are seen between perforation geometries.

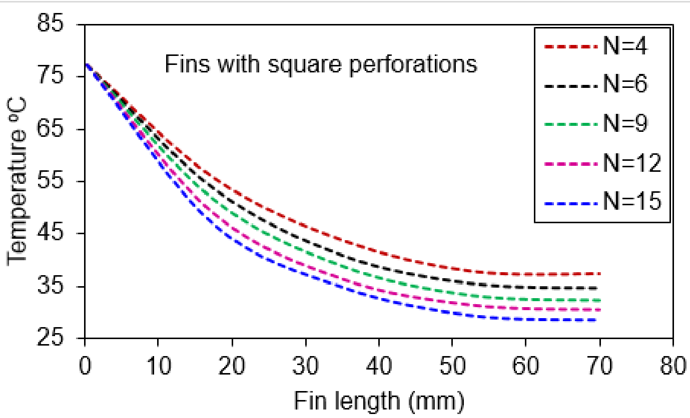

Figure 8. Axial temperature for circular perforations (N = 6, 1.2 m s^{-1}

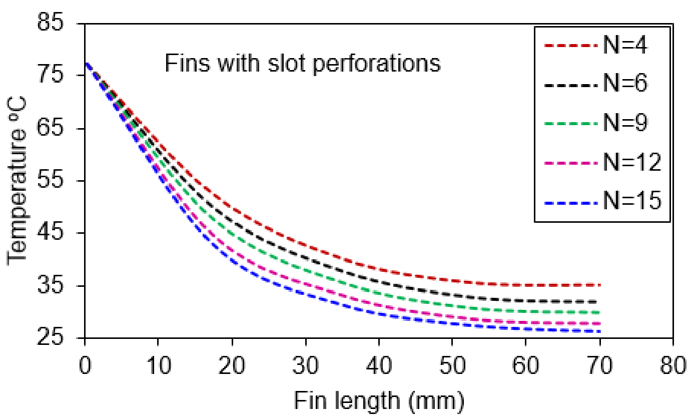

Figure 9. Square perforations under identical conditions

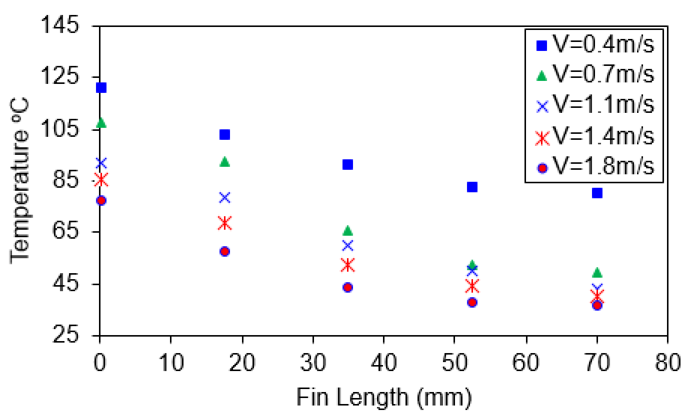

Figure 10. Slot perforations highlight elongated cooling zones

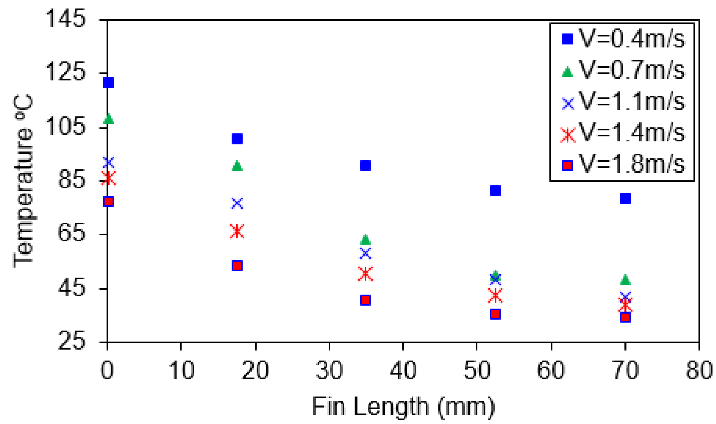

Figure 11. Temperature and velocity correlations

Circular perforations (Figure 8) produce relatively symmetric flow patterns with moderate mixing, while square and rectangular perforations (Figures 9 and 10) generate stronger flow separation and more complex wake structures. These effects arise from sharp edges, which promote shear-layer instability and vortex formation.

As a result, rectangular and slot perforations show enhanced convective heat transfer compared to circular configurations. This is consistent with the observed increase in Nusselt number for these geometries.

Figure 11 illustrates the effect of increasing airflow velocity. Higher velocities intensify convective transport, leading to a reduction in surface temperature and a more uniform temperature distribution along the fin. Quantitatively, the largest surface temperature decreases by approximately 12–18 K in optimized configurations compared to the solid fin baseline.

Additionally, the presence of perforations creates localized cooling regions downstream of each opening. These regions extend approximately two to three perforation diameters and are associated with vortex-induced mixing. Rectangular perforations generate longer wake regions compared to circular ones, which explains their superior thermal performance.

3.6. Interaction between geometry and flow parameters

The combined influence of airflow velocity and perforation geometry plays a critical role in deciding overall performance. While increasing velocity enhances global convective transport, geometric modifications affect local flow behavior.

At low velocities, the effect of perforations is limited due to weaker flow mixing. As velocity increases, the interaction between flow inertia and perforation-induced disturbances becomes more pronounced, resulting in greater heat transfer enhancement.

However, increasing perforation number beyond a certain threshold leads to diminishing returns. Although added perforations increase mixing, they also reduce structural material and may weaken the fin. The results show that perforation counts above approximately N=12 provide only marginal thermal benefit while increasing pressure drop.

This observation highlights the importance of balancing geometric complexity with flow conditions, rather than maximizing a single parameter.

3.7. Uncertainty analysis and robustness

The robustness of the optimized configurations was evaluated using Monte Carlo uncertainty propagation. Variations in airflow velocity, perforation diameter, and thermal conductivity were considered within realistic tolerance ranges.

The results (Table 3) show that the optimized configuration keeps stable performance, with a mean Nusselt number of approximately 66.2 and a 95% confidence interval of (64.1, 67.8). Similarly, the pressure drops stay within a narrow range of (11.1, 13.2) Pa.

Table 3. 95% Confidence Intervals

Metric	Mean Value	95% CI
Nusselt Nu	~66.2	(64.1, 67.8)
Pressure Drop	~12.3 Pa	(11.1, 13.2) Pa

These results show that the optimized designs are not highly sensitive to small variations in operating conditions or manufacturing tolerances. This robustness enhances the practical applicability of the proposed optimization framework.

3.8. Engineering implications

The results prove that perforated fin design involves a trade-off between thermal performance, pressure loss, and structural considerations. The proposed framework enables systematic identification of best configurations based on these competing factors.

From an engineering perspective:

- Airflow velocity is the primary driver of performance and should be carefully controlled
- Rectangular perforations provide improved heat transfer but increase pressure drop
- Moderate perforation density offers a balanced design solution
- Material reduction contributes to weight savings without significantly compromising performance

These findings are particularly relevant for applications such as electronics cooling and aerospace thermal systems, where both thermal efficiency and weight reduction are critical.

4. Conclusion and future work

4.1. Conclusion

This study presented an integrated computational framework for the analysis and optimization of perforated fins under forced convection. The approach combined high-fidelity CFD simulations with Radial Basis Function Neural Network (RBFNN) surrogate modeling and multi-objective optimization using NSGA-II, supported by global sensitivity analysis and uncertainty quantification.

The developed surrogate model proved high predictive accuracy in reproducing CFD results within the investigated parameter space, enabling efficient exploration of the design space without the need for repeated numerical simulations. It is important to emphasize that the validation conducted in this study is limited to numerical consistency with CFD results and comparison with previously published experimental trends [4], and does not constitute direct experimental validation.

The multi-objective optimization results revealed a clear trade-off between heat transfer enhancement and pressure drop. The Pareto front found a range of possible solutions, from high-performance configurations with enhanced heat transfer and increased pressure loss to low-resistance configurations with reduced thermal performance. An optimized configuration achieved approximately 16% improvement in heat transfer compared to a solid fin baseline, while reducing material usage by about 24%.

Sensitivity analysis showed that airflow velocity is the dominant parameter governing thermal performance, contributing approximately 60% to the variation in Nusselt number. Geometric parameters, including perforation diameter and number, primarily influence local flow structures and provide secondary contributions to overall performance. These findings highlight the importance of considering both flow conditions and geometric design in perforated fin optimization.

The uncertainty analysis proved that the optimized configurations keep stable performance under realistic variations in operating conditions and material properties. This robustness supports the practical relevance of the proposed framework for engineering applications.

Overall, the study provides a structured method for evaluating and perfecting perforated fin designs, enabling informed decision-making based on competing thermal and hydraulic aims. The framework can be extended to other thermo-fluid systems where similar trade-offs are present.

4.2. Limitations

Despite the promising results, several limitations should be acknowledged.

First, the CFD simulations are based on steady-state Reynolds-Averaged Navier–Stokes (RANS) modeling using the RNG k–ε turbulence model. While this approach provides a reasonable balance between computational cost and accuracy, it may not fully capture transitional flow behavior or unsteady vortex dynamics, particularly in regions downstream of perforations.

Second, the validation of the surrogate model is limited to numerical data generated by CFD simulations and comparison with previously published experimental studies. The absence of dedicated experimental validation restricts the generalization of the results beyond the investigated parameter space.

Third, the optimization framework focuses on thermo-fluid performance and material reduction without explicitly incorporating structural integrity, manufacturing constraints, or mechanical stresses. These factors may influence the feasibility of certain optimized configurations in real-world applications.

Finally, the surrogate model is trained within a bounded design space. Predictions outside these parameter ranges may lead to reduced accuracy due to extrapolation limitations.

4.3. Future work

Based on the identified limitations and findings, several directions for future research are proposed.

1. Experimental Validation: Conduct controlled experiments on selected Pareto-optimal configurations to validate CFD predictions and surrogate-based optimization results. Techniques such as infrared thermography and detailed temperature measurements can be used to capture heat transfer characteristics.
2. Advanced Turbulence Modeling: Extend the numerical analysis using higher-fidelity approaches such as Large Eddy Simulation (LES) or hybrid RANS–LES models to better capture unsteady flow structures and vortex dynamics induced by perforations.
3. Multi-Physics Optimization: Incorporate structural and mechanical constraints into the optimization framework, including stress analysis, deformation limits, and smallest ligament width, to ensure manufacturability and mechanical reliability.
4. Alternative Surrogate Models: Compare the performance of RBFNN with other surrogate modeling techniques, such as Gaussian Process Regression, Support Vector Regression, and deep neural networks, to evaluate differences in prediction accuracy and computational efficiency.
5. Adaptive Sampling Strategies: Implement active learning or adaptive sampling methods to improve dataset efficiency by selectively generating CFD data in regions of high uncertainty or strong nonlinearity.
6. Transient and Dynamic Conditions: Investigate the performance of perforated fins under transient thermal loads and time-dependent flow conditions, which are relevant for applications such as electronics cooling and energy systems.
7. Extended Geometrical Configurations: Explore more complex perforation patterns and advanced manufacturing approaches, including additive manufacturing, to enable novel geometries that cannot be achieved using conventional fabrication techniques.
8. Scale-Up and Industrial Applications: Apply the proposed framework to full-scale heat exchanger systems, such as plate-fin or tube-fin configurations, to evaluate scalability and industrial applicability.

Author contributions statement

The first author Wadhah Hussein Al Doori contributed conceptualization, method, software, and author Hasan Koten contributed method, software, formal analysis and other sections.

Declaration of interests

The authors have no competing financial or personal interests related to this work.

Data availability

Data availability is available on request.

Declaration of generative ai and ai-assisted technologies in the writing process

No generative AI or AI-assisted technologies were used in the writing manuscript.

Nomenclature

u	Velocity (m/s)
Re	Reynolds number (–)
Nu	Nusselt number (–)
ΔP	Pressure drop (Pa)
d	Perforation diameter (mm)
N	Number of perforations (–)
k	Thermal conductivity (W/m·K)
μ	Dynamic viscosity (Pa·s)
ρ	Density (kg/m^3)
c_p	Specific heat (J/kg·K)

References

[1] L. L. Hein and M. V. V Mortean, “Experiments and Numerical Investigations for Heat Transfer from a Horizontal Plate via Forced Convection Using Pin Fins with Different Hole Numbers,” CFD Letters, vol. 14, no. 9, pp. 1–14, 2022.

[2] W. H. Al Doori, “Numerical estimation of pressure drop and heat transfer characteristics in annular-finned channel heat exchangers with different channel configurations,” Heat Transfer—Asian Research, vol. 48, no. 4, pp. 1280–1291, 2019.

[3] W. H. A. Al-Taha, “Effect of the circular perforations on the heat transfer enhancement by the forced convection from the rectangular fins,” Diyala Journal of Engineering Sciences, vol. 11, no. 3, pp. 62–70, 2018.

[4] T. K. Ibrahim, A. T. Al-Sammarraie, M. S. M. Al-Jethelah, W. H. Al-Doori, M. R. Salimpour, and H. Tao, “The impact of square shape perforations on the enhanced heat transfer from fins: Experimental and numerical study,” International Journal of Thermal Sciences, vol. 149, p. 106144, 2020.

[5] U. V Awasarmol, A. T. Pise, J. D. Patil, L. D. Jathar, and R. R. Verma, “Experimental investigation of heat transfer enhancement by using perforated fin array having different perforation ratios, angle of inclination and configuration of fins under forced convection condition,” International Communications in Heat and Mass Transfer, vol. 147, p. 106995, 2023.

[6] O. N. Sara, T. Pekdemir, S. Yapici, and M. Yilmaz, “Heat-transfer enhancement in a channel flow with perforated rectangular blocks,” International Journal of Heat and Fluid Flow, vol. 22, no. 5, pp. 509–518, 2001.

[7] W. H. A. R. Al Taha, “Analysis, Performance and Optimization of Perforated and Non-Perforated Fins under Forced Convection.” Sudan University of Science and Technology, 2018.

[8] N. Sözbir and İ. Ekmekçi, “Experimental study and artificial neural network modeling of unsteady laminar forced convection in a rectangular duct,” Heat and mass transfer, vol. 43, no. 8, pp. 749–758, 2007.

[9] G. N. Xie, Q. W. Wang, M. Zeng, and L. Q. Luo, “Heat transfer analysis for shell-and-tube heat exchangers with experimental data by artificial neural networks approach,” Applied Thermal Engineering, vol. 27, no. 5–6, pp. 1096–1104, 2007.

[10] A. Tandiroglu, “Artificial neural network approach for transient forced convective heat transfer optimization,” Int J Mech Eng Appl, vol. 4, no. 6, pp. 212–225, 2016.

[11] R. Romero-Méndez, P. Lara-Vázquez, F. Oviedo-Tolentino, H. M. Durán-García, F. G. Pérez-Gutiérrez, and A. Pacheco-Vega, “Use of artificial neural networks for prediction of the convective heat transfer coefficient in evaporative mini-tubes,” Ingeniería, investigación y tecnología, vol. 17, no. 1, pp. 23–34, 2016.

[12] Y. Varol, E. Avci, A. Koca, and H. F. Oztop, “Prediction of flow fields and temperature distributions due to natural convection in a triangular enclosure using Adaptive-Network-Based Fuzzy Inference System (ANFIS) and Artificial Neural Network (ANN),” International Communications in Heat and Mass Transfer, vol. 34, no. 7, pp. 887–896, 2007.

[13] X. Xu, S. Ding, Z. Shi, and H. Zhu, “Optimizing radial basis function neural network based on rough sets and affinity propagation clustering algorithm,” Journal of Zhejiang University SCIENCE C, vol. 13, no. 2, pp. 131–138, 2012.

[14] A. Barati-Harooni, A. Najafi-Marghmaleki, and A. H. Mohammadi, “A reliable radial basis function neural network model (RBF-NN) for the prediction of densities of ionic liquids,” Journal of Molecular Liquids, vol. 231, pp. 462–473, 2017.

[15] L. Cao et al., “Optimization of processing parameters of AISI 316L laser welding influenced by external magnetic field combining RBFNN and GA,” Results in physics, vol. 7, pp. 1329–1338, 2017.

[16] M. Kavitha, L. B. Abhang, M. Kumar, M. Balamurugan, and M. P. Mallesh, “Advanced Finite Element Methods for Solving Fluid Dynamics Problems in Engineering Applications,” Metallurgical and Materials Engineering, vol. 31, no. 3, pp. 201–209, 2025.

[17] C. Zhang and C. Luo, “Analysis of heat transfer and flow performance in elliptical perforated fin heat exchangers,” Journal of Thermal Analysis and Calorimetry, vol. 150, no. 18, pp. 14687–14699, 2025.

[18] M. I. Hossain, M. S. H. Chowdhury, S. S. U. Ahmed, A. Hamja, and I. J. Siddique, “Forced convective heat transfer over twisted and perforated forked pin fin heat sink: A numerical study,” International Journal of Thermal Sciences, vol. 211, p. 109719, 2025.

[19] A. F. Saeed and N. Raad, “Numerical and experimental analysis of thermal transfer for radial-shaped holed fins,” Ain Shams Engineering Journal, vol. 16, no. 9, p. 103529, 2025.

[20] F.-T. Zohora, M. R. Haque, N. M. Chowdhury, M. K. Fahad, and N. F. Ifraj, “Optimization of hydrothermal performance in industrial heat sinks with innovative perforated pin fin designs: A numerical approach,” Heliyon, vol. 11, no. 1, 2025.

[21] A. Yusuf and M. M. Bhatti, “Coupled nonthermal plasma and photocatalytic surface reactions in mass-based ZnO-Au/water hybrid nanofluid flow,” International Journal of Heat and Fluid Flow, vol. 117, p. 110087, 2026.

[22] W. H. A. Al Doori and A. M. Hussien, “Safe Energy using Hydraulic System Analysis at a Hydropower Plant,” Journal of Advanced Research in Fluid Mechanics and Thermal Sciences, vol. 116, no. 2, pp. 131–143, 2024.

[23] Bhatti, M. M., & Rashidi, M. M. (2016). Effects of thermo-diffusion and thermal radiation on Williamson nanofluid over a porous shrinking/stretching sheet. Journal of Molecular Liquids, 221, 567-573.

[24] M. R. Shaeri, M. Yaghoubi, and K. Jafarpur, “Heat transfer analysis of lateral perforated fin heat sinks,” Applied energy, vol. 86, no. 10, pp. 2019–2029, 2009.